OM-DS-SS WIRELESS LAN RADIO SUBSYSTEM: PERFORMANCE IN CLIPPING ENVIRONMENT USING MEASURED CHANNEL DELAY PROFILES

Paolo Banelli, Saverio Cacopardi, Fabrizio Frescura, Gianluca Reali

Istituto di Elettronica, Università di Perugia -Via G. Duranti 1 - 06125 Perugia - Italy

e-mail: banelli@istel.ing.unipg.it cacopar@istel.ing.unipg.it - frescura@istel.ing.unipg.it - reali@istel.ing.unipg.it

ABSTRACT This paper investigates a new radio access scheme, based on Orthogonal Multicarrier DS-SS, for WLAN. The modem scheme, the sounding and equalisation techniques and the general format of the frame for various system configurations are presented, taking a realistic sounding technique into consideration. We report the analytical bit error rate performance and the simulation results, based on a measured set of indoor channel delay profiles, for both linear and ideal pre-distorted non-linear amplifiers (i.e. soft limiters). The analysis of clipping effect in the non-linear environment allows us to specify the minimum back-off value for the various system configurations in order to balance the bit error rate performance and the efficiency of power amplifiers. Moreover the obtained performance constitutes a lower bound reference for performance evaluation of pre-distortion schemes.

1. Introduction

Within the present trend in telecommunications towards the introduction of mobility, whenever market interest and technical solutions exist, the new generation of multimedia services supported by laptop and palmtop computing devices lead directly to the development of high speed Wireless Local Area Networks (WLANs). Mobility, however, is always a difficult feature to be delivered, especially when it involves a challanging transmission medium such as the indoor radio channel. The only standards delivered by regulatory bodies are the ETSI HIPERLAN and the IEEE 802.11 [1][2][3]. They are attempts, strongly solicited by manufacturers, to create order within a framework characterized by separated technical solutions, without neither network nor service interworking.

Interference is a further problem that affects WLANs. In fact WLAN applications are often established using bands where electronic devices radiate RF energy (e.g. ISM). In this challenging environment the interference rejection properties of the Spread Spectrum (SS) technique are precious. Moreover, the SS offers an effective capability to combat the well known multipath phenomenon [4]. In this paper we show the convenience to combine the SS signalling with the Orthogonal Multicarrier (OM) modulation in order to support indoor WLAN applications. This approach permits to displace equalisation problems from the time domain to the frequency domain [5]. As a consequence, it leads to different technical solutions, such as full equalisation of the channel by means of a Complex-values Automatic Gain Control (CAGC), that could result attractive from the point of view of hardware and computational costs [6][7][8]. However, all considerations are valid only if they reflect real system behavior during operation. With this in mind, we carry out the analysis by using measured channel delay profiles, which represent an heavy multipath phenomenon, and point out the potential performance limiting factors. For instance, since the technique that we are going to present produce non-constant signal envelope, non linear effects within the transmission chain endanger the system performance seriously. Non linear effects are primarily due to amplifier characteristics and clipping processes [9][10]. In this paper we evaluate the system performance when amplifiers work both in the linear region and when they are pushed in saturation. In this second case, in order to find the irreducible effects of such a problem, ideal pre-distortion schemes are adopted. This problem is faced by means of a clipping process that schematizes the ideal pre-distortion of the power amplifier. We show that even if the pre-distortion is optimal, the clipping effect has a sensitive impact on system performance. We first present an analytical approach, then verify the results obtained by means of simulation trials.

II. Radio Subsystem Description

II.1 Modem Scheme

Fig. 1 shows the basic schemes of the TX and RX base-band sections of the OM-DS-SS modem considered. We start describing the scheme from the transmitter.

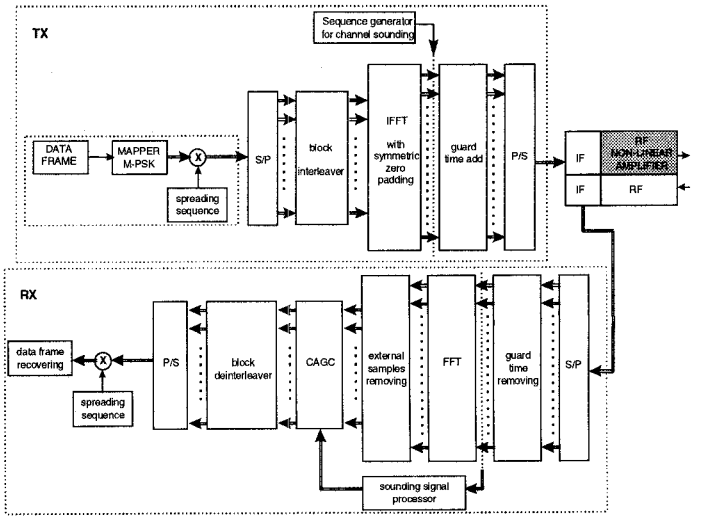

Fig. 1 Basic schemes of the TX and RX base-band sections of the OM-DS-SS modem. Double lines indicate complex-valued signals.

0-7803-3336-5/96 $5.00 © 1996 IEEE

The data frame is packed into blocks of μm bits. Each block is then mapped into μ symbols of the M-PSK constellation (with $M=2^m$) according to the Gray code. The resulting complex-valued block is spread by μ periods of a unique spreading sequence. We denote by L the period of the sequence. The spread block is serial to parallel converted in a vector of μL components and then scrambled by a block interleaver of depth equal to μ. The resultant vector feeds an IFFT processor which operates on $L_{fft} > \mu L$ samples. In particular, each vector is padded by $N_1 = \lfloor (L_{fft} - \mu L)/2 \rfloor$ and $N_2 = L_{fft} - N_1$ zeros at its edges. This operation allows it to avoid spectral overlapping at the receiver side. When the sequence generator provides the sounding signal, the IFFT processor and the functional blocks that precede it are being bypassed. Since the system operates in a frequency-selective fading environment, guard times of duration T_g larger than the delay spread of the channel are added between adjacent IFFT transformed vectors. The guard time avoids inter-symbol interference (ISI) and inter-carrier interference (ICI) at the receiver. The resulting vector, after a parallel to serial conversion, feeds the IF-RF sections.

The receiver section of the modem in Fig. 1 is in some way dual with respect to the transmitter with the exception of the Complex-values Automatic Gain Control (CAGC) functional block. From the RF-IF section the received signal is sampled and serial to parallel converted; then the guard time is removed. During the sounding of the channel, the signal is picked up at the input of the FFT processor and is processed to derive the CAGC coefficients. In a different way, during the reception of the blocks corresponding to the data frames, the receiver performs an FFT processing on L_{fft} samples, eliminates the zeros at the edges of the received vector to extract the μL central components, and then processes the resulting vector by means of the CAGC and the deinterleaver. After a parallel to serial conversion the signal feeds the spread spectrum receiver and then the data recovering circuits.

II.2 Sounding and Equalisation Techniques

A set of indoor measurements in different environments has been performed by CSELT using wide-band equipment (20 MHz) in the 2 GHz frequency band. All the measurements were performed along a track of 3 m, sampled at a spatial resolution of $\lambda/8$ (λ being the wavelength). Starting from a transmitted signal $x(t)$ and a received one $y(t)$, for each different spatial position along the track, the complex channel transfer function can be obtained as

$$H^*(f,s) = S_{xy}(f,s)/S_{xx}(f,s) \tag{1}$$

where $S_{xy}(f,s)$ is the cross spectral density between the signals $x(t)$ and $y(t)$, $S_{xx}(f,s)$ the power spectrum of $x(t)$ (s denoting the spatial position). From the channel transfer function in the frequency-spatial domain, the complex impulse response can be derived as follows:

$$h(\tau,s) = F_f^{-1}\{H(f,s)\} \tag{2}$$

where the operator $F_f^{-1}\{\cdot\}$ is the inverse Fourier transform in the frequency domain. According to the so-called *discrete multipath time-domain model*, which describes the channel as a linear space-variant filter, the received signal can be written as

$$r(t) = \sum_{p=1}^{N_p} h(pT_S, s) S(t - pT_S) + n(t) \tag{3}$$

were T_S is the time duration of the transmitted samples, $S(t)$ is the transmitted signal, N_p is the number of paths of the channel, $h(pT_s, s)$ is the space-variant complex-valued coefficient that corresponds to the pth path, $n(t)$ is the Additive White Gaussian Noise (AWGN). The maximum value of the time delay N_pT_S, represents the channel *delay spread*. Because of the small random variations of the environment and the user mobility, the space-variant nature of the channel translates itself in a time dependence of the channel impulse response. If the duration $T_b = L_{fft}T_S$ of the transmitted OM symbols (L_{fft} components) is considerably smaller than the coherence time ($\Delta T_c = 1/f_D$, f_D being the maximum Doppler frequency) of the channel, the slow fading channel condition is maintained. Therefore, expression (3) can be written as

$$\mathbf{R} = \mathbf{h} * \mathbf{S} + \mathbf{N} \tag{4}$$

In (4) the symbol "*" denotes the linear discrete convolution, $\mathbf{S} = [s_1, s_2, \ldots, s_{L_{fft}}]$ is the transmitted vector (both sounding or data), $\mathbf{h} = [h_1, h_2, \ldots h_{N_p}] = [h(T_S,s), h(2T_S,s) \ldots h(N_pT_S,s)]$ is the discrete channel impulse response at the sounding time, $\mathbf{N} = [n_1, n_2, \ldots, n_{L_{fft}+N_p-1}]$ is the AWGN vector and $\mathbf{R} = [r_1, r_2, \ldots, r_{L_{fft}+N_p-1}]$ is the corresponding received one.

Because of the presence of noise, the more powerful the transmitted sounding blocks are, the more accurate the channel estimation is. The sounding vector consists in a train of pulses, time-spaced, at least, by the channel *delay spread* [11]. The sounding generator provides the following sequence:

$$B_s[k] = \sqrt{\frac{\gamma}{P}} \sum_{n=0}^{P-1} \delta\left(k - n\left(N_p + 1\right)\right), \quad 1 \le k \le L_{fft}, \tag{5}$$

where $\begin{cases} \delta(k) = 1, & k = 0 \\ \delta(k) = 0, & k \neq 0, \end{cases}$ (6)

$P = \lfloor L_{fft} / (N_p + 1) \rfloor$ is the number of pulses in each sounding vector and γ is the energy value of the sounding vector. For this purpose we denote as S/D the energy ratio between the sounding and the data vectors.

The receiver processes the corresponding received signal

$$\mathbf{R}_s = \mathbf{h} * \mathbf{B}_s + \mathbf{N} \tag{7}$$

by segmenting $\mathbf{R}_s$ in P sub-blocks of $N_p + 1$ samples

$$\mathbf{R}_s^{(i)} = \mathbf{R}_s\left[(i-1)(N_p+1)+1, .., i(N_p+1)\right], \quad i = 1, .., P. \tag{8}$$

To obtain an estimation of the channel impulse response, the

sub-blocks (8) are averaged as follows:

$$\tilde{\mathbf{h}} = \left[\tilde{h}_1, \tilde{h}_2, \ldots, \tilde{h}_{N_p+1}\right] = \frac{\left(1/\sqrt{\gamma/P}\right)\sum_{i=1}^{P} \mathbf{R}_s^{(i)}}{P} \quad . \tag{9}$$

After a zero padding of the vector (9) up to L_{fft} samples, its FFT provides $\tilde{\mathbf{H}} = [\tilde{h}_1, \tilde{h}_2, \ldots \tilde{h}_{L_{fft}}]$, which represents the estimation of the channel transfer function.

From the estimated channel response $\tilde{\mathbf{H}}$, the CACG coefficients are obtained by the conjugate of each component (i.e. Maximum Ratio Combining)

$$C[k] = \tilde{H}^*[k], \quad k = N_1 + 1, \ldots, L_{fft} - N_2 \tag{10}$$

This technique recovers the phase shift due to the channel, but alters the magnitude; this approach produces excellent performance in single user operation since noise amplification is avoided, but leads to a very poor performance in multi-user applications as the orthogonality properties of the spreading sequence get lost [6][11][12]. This fact does not represent a drawback in WLAN applications, since a CSMA/CA (Carrier Sense Multiple Access with Collision Avoidance) access scheme is generally adopted.

II.3 Model of ideal pre-distorted power amplifiers

A non-linear power amplifier can be modelled as a memoryless device [13]. If the signal at the input of a non linear amplifier is expressed by its complex base-band representation

$$s(t) = R(t) \cdot e^{j\vartheta(t)} \tag{11}$$

the non linear distorted output is

$$s_d(t) = H[R(t)] \cdot e^{j[\vartheta(t) + \Phi[R(t)]]} \tag{12}$$

where $H[R]$ and $\Phi[R]$ are indicated as AM/AM and AM/PM distortion curves respectively.

A well known technique for counteracting the non linear distortion of the RF power amplifier consists in the base-band pre-distortion of the magnitude $R(t)$ of the input signal by two curves $G[R]$ and $\Psi[R]$ that invert $H[R]$ and $\Phi[R]$ [13]. The overall system formed by the cascade of the pre-distortion device and the non-linear amplifier may be modelled ideally as a soft-limiter device, which corresponds to an AM/PM perfect cancellation and an AM/AM reduction to a simple clipping distortion because of the maximum allowed output power of the amplifier.

Since the AM/AM and AM/PM depends on the signal magnitude $R(t)$ only, in the following we refer to the magnitude clipping of the signal; it has different impact on the signal distortion with respect to the clipping introduced on I and Q signal components by the A/D - D/A conversion process present in the system [14].

The complex base-band representation of the L_{fft} OM signal samples transmitted during each period $T_b = L_{fft} T_S$ is [8]:

$$\hat{S}[n] = s[n] + j s_H[n] = IFFT\left\{\hat{z}_k\right\} = \sum_{k=0}^{L_{fft}-1} \hat{z}_k e^{j\frac{2\pi}{N}kn}, \; n = 0, \ldots, L_{fft} - 1 \tag{13}$$

where $\hat{z}_k = a_k + jb_k$ represents the unmodulated complex information symbols. If the real symbols a_k and b_k are statistically independent, the number of the carriers L_{fft} is large enough, and the power is uniformly distributed on each carrier, $s[n]$ and $s_H[n]$ are gaussian distributed with cross-correlation

$$R_{S,S_H}[n] = \sigma_o^2 \sum_{k=0}^{L_{fft}-1} \sin\left(\tfrac{2\pi}{L_{fft}} nk\right) = 0, \; L_{fft} \; even, \; \forall n \tag{14}$$

where $\sigma_o^2 = E\left\{a_k^2\right\} = E\left\{b_k^2\right\}$ is the power of each carrier.

Under these hypothesis, the magnitude $R[n] = \sqrt{s^2[n] + s_H^2[n]}$ of the complex base band signal $\hat{S}[n]$ is Rayleigh distributed:

$$p(R) = \frac{R}{\alpha} e^{-\frac{R^2}{2\alpha^2}}, \qquad R > 0 \tag{15}$$

where $E\left\{|\hat{S}|^2\right\} = 2E\left\{S^2\right\} = 2\alpha^2$ represents the mean power of the complex base-band OM signal. The effect of magnitude clipping is both the distortion of the output signal and the reduction of its mean power [15]. If $g(.)$ is the input-output characteristic of the clipper and $R_c = g(R)$ is the magnitude of the output clipped complex signal $\hat{S}_c$, the mean power at the output is easily obtained as

$$\begin{aligned} E\left\{\left|\hat{S}_c\right|^2\right\} &= E\left\{R_c^2\right\} = \int_0^\infty g^2(R) p(R) dR = \int_0^A R^2 p(R) dR + \int_A^\infty A^2 p(R) dR \\ &= 2\alpha^2\left(1 - e^{-A^2/2\alpha^2}\right) = E\left\{|\hat{S}|^2\right\} \cdot \left(1 - e^{-c^2/2}\right) = E\left\{|\hat{S}|^2\right\} \cdot \Gamma(IBO), \end{aligned} \tag{16}$$

$c = A/\alpha$ being the so called '*clipping ratio*', $IBO = c^2/2$ the Input Back-Off of the pre-distorted power amplifier and $\Gamma(IBO) = 1 - e^{-IBO}$ the power attenuation of the signal.

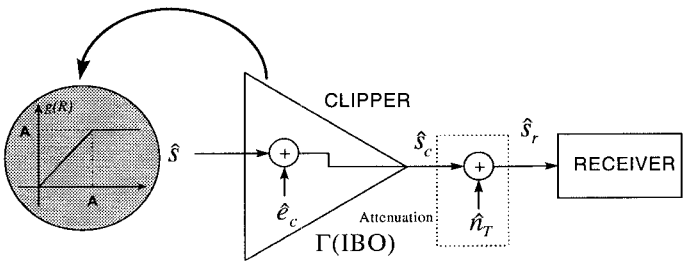

Fig. 2 General clipping model for OM communication systems.

The clipping input-output error is introduced as

$$\hat{e}_c[n] = \hat{s}[n] - \hat{s}_c[n] = \begin{cases} 0 & \text{for } |\hat{S}| > A \\ (R[n] - A) e^{j\vartheta[n]} & \text{for } |\hat{S}| > A \end{cases} \tag{17}$$

with mean value equal to zero ($\vartheta[n] = \tan^{-1}\left(s_H[n]/s[n]\right)$ being uniformly distributed in $[0, 2\pi]$) and mean power given by:

$$\sigma_e^2 = E\left\{|\hat{e}_c|^2\right\} = E\left\{R_e^2\right\} = \int_0^\infty R_e^2\, p\left(R\right) dR = \int_A^\infty (R-A)^2\, p(R) dR$$
$$= E\left\{|S|^2\right\}\cdot\left[e^{-c^2/2} - \sqrt{\tfrac{\pi}{2}}\cdot c\cdot erfc\left(c/\sqrt{2}\right)\right] = \quad (18)$$
$$= E\left\{|S|^2\right\}\cdot\left[e^{-IBO} - \sqrt{\pi\, IBO}\cdot erfc\left(\sqrt{IBO}\right)\right] = E\left\{|S|^2\right\}\cdot F(IBO)$$

where $erfc(x)$ is the complementary error function

$$erfc(x) \equiv 1 - \frac{2}{\sqrt{\pi}}\int_0^x e^{-t^2} dt\,. \quad (19)$$

In the following, the power spectrum of the clipping noise is assumed to be flat and totally contained within the signal bandwidth. This hypothesis corresponds to a clipping of the signal without interpolation. Otherwise, in the case of signal interpolation, the error power is generally spread over a band wider than the useful transmit band [16]. However, we may consider the performance obtained by means of the above hypothesis as an upper bound with respect to the case of interpolated clipping.

By means of (16) and (18) the clipper can be modelled, for an OM system, like a device that adds to the input signal a (correlated) error signal and attenuates the total power by a factor equal to Γ(IBO), as shown in Figure 2. In this figure an ideal AWGN channel is assumed. The SNR at the receiver side, in clipping AWGN environment, may be defined as [15]

$$(SNR)_{clip}^{AWGN} = \frac{E\left\{\left|\hat{S}_c\right|^2\right\}}{E\left\{\left|\hat{e}_c\right|^2\right\} + \sigma_{n_T}^2} \quad (20)$$

Making use of (16) and (18), expression (20) becomes

$$(SNR)_{clip}^{AWGN} = \frac{\Gamma(IBO)}{F(IBO) + \sigma_{n_T}^2 / E\left\{|S|^2\right\}} = \frac{\Gamma(IBO)}{F(IBO) + 1/(SNR)_{lin}^{AWGN}} \quad (21)$$

whose shape is shown in Fig. 3.

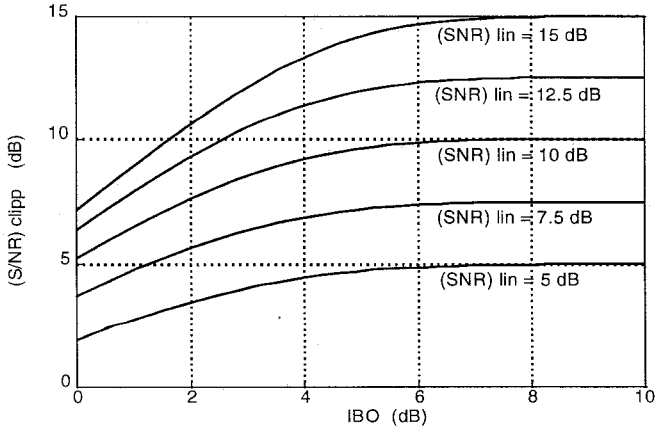

Fig. 3 Penalty in term of SNR for an amplitude limited OM communication system.

When BER performance in AWGN channel of an OM system without clipping is known for a certain $(SNR)_{lin}^{AWGN}$, the corresponding performance in clipping environment is predictable simply substituting in the BER curve the value of the $(SNR)_{clip}^{AWGN}$ corresponding to the desired IBO.

II.4 Frame Description

Fig. 4 shows the frame structure of the proposed OM-DS-SS radio access scheme for 4-PSK and 8-PSK data mapping. The transmitted blocks, both sounding and data, are 2048 samples long. The data blocks contain 169 symbols, each spread by a period of an 11 chip Barker sequence. In the case of 4-PSK mapping, a frame of 2366 bytes is segmented into 56 blocks. A sounding block is transmitted at the beginning of the frame and every 14 data blocks. In the second application case the 8-PSK mapping is used. A frame of 2471 bytes is segmented into 39 blocks. The sounding block is transmitted at the beginning of the frame and interleaved every 13 blocks.

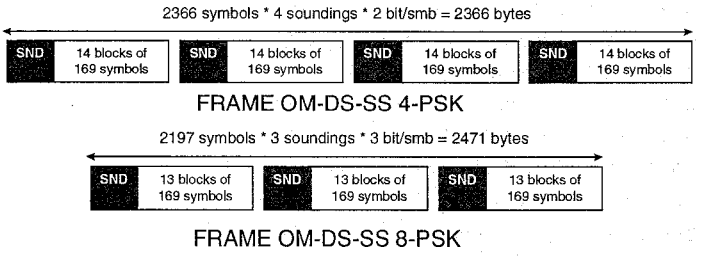

Fig. 4 General frame format of the OM-DS-SS radio access scheme.

Table 1 shows some system parameters of the OM-DS-SS radio access schemes.

	OM-DS-SS 4-PSK	OM-DS-SS 8-PSK
Sample Rate	20 Msample/s	20 Msample/s
Symbol Rate	1.5 Mbaud	1.5 Mbaud
Spreading	11 chip Barker	11 chip Barker
Bit Rate	3 Mbit/s	4.5 Mbit/s
Max. Frame Length	2366 bytes	2471 bytes
OM Block Duration T_B	(*) 1.00E-4 s	(*) 9.98E-5 s
OM Frame Duration	60 * T_B	42 * T_B

***Table 1:** System parameters of the OM-DS-SS WLAN. (*) A guard time of 22 chips corresponding to 1.1 ms is included.*

From the observation of the values reported in the table it is evident the overhead due to the sounding, to the guard time and to the guard band in the OM-DS-SS technique. The introduced overhead reduces the achievable bit rate by about 18%.

III. Performance Analysis

Relation (4) represents the signal expression, in the time domain, at the receiver side. During the transmission of data blocks the signal vector **S** is given by

$$\mathbf{S} = [s_1, s_2, \ldots s_{L_{fft}}] = IFFT\{\mathbf{D}\},$$
$$\mathbf{D} = [\underbrace{0,0,..,0}_{N_1}, d_1, d_2, \ldots, d_{\mu L}, \underbrace{0,0,\ldots,0}_{N_2}], \quad (22)$$

D being the spread, interleaved and zero-padded data vector. Provided that the guard time T_g is correctly sized in order to avoid ICI and ISI, after the FFT processor each received vector

is given by

$$\mathbf{R}_{fft} = [R_1, R_2, ..., R_{L_{fft}}] = FFT\{\mathbf{R}\} = \mathbf{H} \otimes \mathbf{D} + \mathbf{N}_{fft} \quad (23)$$

In (23) the symbol "$\otimes$" denotes a component by component complex-valued multiplication, $\mathbf{H} = [H_1, H_2, ... H_{L_{fft}}]$ is the channel frequency response, and $\mathbf{N}_{fft} = [N_1, N_2, ..., N_{L_{fft}}]$ is the FFT transformed AWGN vector. In other words each component of the data vector $\mathbf{D}$ is multiplied by a complex-valued coefficient, viz. a sample of the instantaneous transfer function of the channel. After the CAGC processing the received signal can be written as

$$\mathbf{Y} = \mathbf{C} \otimes \mathbf{R}_{fft} = \mathbf{C} \otimes \mathbf{H} \otimes \mathbf{D} + \mathbf{C} \otimes \mathbf{N}_{fft},$$
$$\mathbf{C} = [\overbrace{\underbrace{0,0,...,0}_{N_1}, c_1, c_2, ..., c_{\mu L}, \underbrace{0,0,...,0}_{N_2}}^{L_{fft}}] \quad (24)$$

where $c_1, c_2, ..., c_{\mu L}$ are calculated according to (10). After the deinterleaving and the despreading of the vector $\mathbf{Y}' = \mathbf{Y}[N_1 + 1, ..., L_{fft} - N_2]$, formed by the μL non-zero components of the vector (24), the detected M-PSK symbols are obtained. In particular, each M-PSK symbol is obtained by a threshold decision of the scalar product of the spreading code and the relative segment of the $\mathbf{Y}'$ vector according to the following:

$$p^{(j)} = trsh\left(\mathbf{b} \bullet \mathbf{y}'_{(j)}\right), \quad \mathbf{y}'_{(j)} = [y'_1, y'_2, ..., y'_L] = \\ = \mathbf{Y}'[(j-1)L+1, ..., jL], \quad j = 1, .., \mu \quad (25)$$

where $p^{(j)}$ is the jth decoded M-PSK symbol, $trsh(.)$ is the threshold decision function, and $\mathbf{b} = [b_1, b_2, ..., b_l, ..., b_L]$, $b_l \in \left\{-1/\sqrt{L}, +1/\sqrt{L}\right\}$ is the spreading sequence. The symbol "$\bullet$" denotes the scalar product.

III.1 System Performance in Linear Environment

To obtain an expression of the BER, we now consider the detection of the generic M-PSK symbol $p^{(j)}$. The scalar product in (25) can be expanded as

$$\mathbf{b} \bullet \mathbf{y}'_{(j)} = \sum_{l=1}^{L} b_l c_l \left(h_l b_l p^{(j)} + n_l\right) = \underbrace{\frac{p^{(j)}}{L} \sum_{l=1}^{L} c_l h_l}_{a} + \underbrace{\sum_{l=1}^{L} b_l c_l n_l}_{b} \quad (26)$$

In (26) the first summation of the right hand side represents the useful signal, while the second summation is due to noise. To take into account the effect on the performance of the channel sounding, the CAGC coefficients c_l can be rewritten as

$$c_l = c'_l + n_l', \quad c'_l = h_l^*, \quad l = 1, ..., L \quad (27)$$

In other words, each coefficient in (27) is modelled as the sum of two contributions. The former is obtained by an ideal sounding operation and its value calculated according to the Maximum Ratio Combining equalisation technique, the latter contribution is a noise term that takes account of the real sounding technique.

By means of (27), expression (26) may be rewritten as

$$\mathbf{b} \bullet \mathbf{y}'_{(j)} = \sum_{l=1}^{L} b_l c_l \left(h_l b_l p^{(j)} + n_l\right) = \underbrace{\frac{p^{(j)}}{L} \sum_{l=1}^{L} c'_l h_l}_{a} + \underbrace{\frac{p^{(j)}}{L} \sum_{l=1}^{L} n'_l h_l}_{a'} + \\ + \underbrace{\sum_{l=1}^{L} b_l c'_l n_l}_{b} + \underbrace{\sum_{l=1}^{L} b_l n'_l n_l}_{b'} \quad (28)$$

The interleaver makes the h_l coefficients, and consequently the c'_l coefficients, independent of the l index, so if we now consider the energy values related to the various contributions in (28), we obtain:

$$(a).\ E_a \cong E_p \mathrm{E}\left\{\left|c'_l h_l\right|^2\right\}, \quad (a').\ E_{a'} \cong E_p \sigma_{n'}^2 \mathrm{E}\left\{\left|h_l\right|^2\right\}$$
$$(b).\ E_b \cong \sigma_n^2 \mathrm{E}\left\{\left|c'_l\right|^2\right\}, \quad (b').\ E_{b'} \cong \sigma_n^2 \sigma_{n'}^2 \quad (29)$$

In (29) E_p is the mean energy value of the M-PSK symbols, σ_n^2 and $\sigma_{n'}^2$ are the variances of the noise related to the data and of the noise related to the sounding, respectively. In particular the value of the variance $\sigma_{n'}^2$ depends on the sounding technique adopted and on the energy of the sounding signal. It may be found that, for the adopted sounding technique and at low values of σ_n^2, the two variances σ_n^2 and $\sigma_{n'}^2$ are related according to the following expression:

$$\sigma_{n'}^2 \cong \frac{1}{S/D} \frac{N_p + 1}{P} \sigma_n^2. \quad (30)$$

The noise contributions (a'), (b) and (b') in (29) are independent and Gaussian. Their sum is a zero-mean Gaussian distribution with a variance equal to the sum of their variances, so, taking into account the threshold decision (25), the BER for the M-PSK scheme [17] is upper bounded by

$$BER|_{M-PSK} \le \frac{1}{\log_2(M)} erfc\left\{sin\frac{\pi}{M}\sqrt{(SNR)_{lin}}\right\},$$
$$(SNR)_{lin} = \frac{E_a}{E_{a'} + E_b + E_{b'}} \quad (31)$$

Expression (31) represents an upper bound for the BER under the hypothesis of time-invariant channel, i.e. the error estimation of the CAGC coefficient values is due only to the noise related to the sounding operation. The time-variant nature of the channel produces a performance penalty which depends on the speed of the mobile user. Nevertheless, in WLAN applications, the typical user's speed is low enough to make expression (31) a good approximation of the performance in operation.

III.2 System Performance in Clipping Environment

In the paragraph II.3 the clipping phenomenon was modelled as an attenuation $\Gamma(IBO)$ of the useful signal power, combined with a noise source, whose variance is given by (18). Moreover, expression (21) of $(SNR)_{clip}$ in AWGN channel was derived.

In this paragraph we derive an expression for $(SNR)_{clip}$ that takes account of the OM-DS-SS system configuration and we modify expression (31) to derive the system performance in clipping conditions and in a measured frequency selective fading channel. Taking account of the clipping effect, the signal after the CAGC operation at the receiver side, may be considered as a combination of the following terms

$$\mathbf{C}\otimes\mathbf{H}\otimes\mathbf{D}_c$$
$$\mathbf{C}\otimes\mathbf{H}\otimes\mathbf{N}_{clipp} \qquad (32)$$
$$\mathbf{C}\otimes\mathbf{N}_{fft}$$

$\mathbf{D}_c$ being the clipped signal, $\mathbf{N}_{clip}=\left[n_1^{clip},n_2^{clip},\ldots,n_{L_{fft}}^{clip}\right]$ a clipping noise vector with variance given by expression (18) scaled by L_{fft}, and $\mathbf{N}_{fft}$ the thermal noise vector. By means of considerations similar to those reported in paragraph III.1, the Sound to Noise Ratio in clipping conditions $(SNR)_{clip}$ may be approximated as

$$(SNR)_{clip}=\frac{E_a^{clip}}{E_{a'}^{clip}+E_b^{clip}+E_{b'}^{clip}+E_c^{clip}+E_{c'}^{clip}}=\frac{\Gamma(IBO)\cdot E_a}{\left[E_{a'}\cdot\Gamma(IBO)+E_b+E_{b'}\right]+E_c^{clip}+E_{c'}^{clip}} \qquad (33)$$

where

$$\begin{aligned}
&(a).\ E_a^{clip} \cong E_{p_c}\,\mathrm{E}\left\{\left|c'_l\,h_l\right|^2\right\}\equiv\Gamma(IBO)\cdot E_p\cdot\mathrm{E}\left\{\left|c'_l\,h_l\right|^2\right\}\equiv\Gamma(IBO)\cdot E_a\\
&(a').\ E_{a'}^{clip} \cong E_{p_u}\sigma_{n'}^2\,\mathrm{E}\left\{\left|h_l\right|^2\right\}\equiv\Gamma(IBO)\cdot E_p\cdot\sigma_{n'}^2\,\mathrm{E}\left\{\left|h_l\right|^2\right\}\equiv\Gamma(IBO)\cdot E_a\\
&(b).\ E_b^{clip} \equiv\sigma_n^2\,\mathrm{E}\left\{\left|c'_l\right|^2\right\}\equiv E_b\\
&(b').\ E_{b'}^{clip}\equiv\sigma_n^2\sigma_n^2\equiv E_{b'}\\
&(c).\ E_c^{clip} \equiv\sigma_{n^{clip}}^2\,\mathrm{E}\left\{\left|c'_l\,h_l\right|^2\right\}\\
&(c').\ E_{c'}^{clip}\equiv\sigma_n^2\sigma_{n^{clip}}^2\,\mathrm{E}\left\{\left|h_l\right|^2\right\}
\end{aligned} \qquad (34)$$

Expression (33) takes account of the OM-DS-SS system configuration, the sounding technique and the equalisation of the fading channel. By substituting the $(SNR)_{lin}$ in expression (31) with $(SNR)_{clip}$ of (33), the BER performance of the OM-DS-SS system are obtained.

IV. Numerical Results

To obtain the performance in linear environment, using the set of measured channel delay profiles described above, the statistical parameters (29) are evaluated numerically. The values are substituted in (31) in order to obtain the BER values for the considered system configurations. Moreover, to confirm the proposed system configurations, simulation trials are performed. The simulation set-up is reported below.

- FFT block length: ***2048 samples***;
- Sounding / Data power ratio (S/D): ***-10dB, -2.5dB, +2.5 dB***
- Carrier frequency: ***2.0 GHz***;
- Maximum Doppler Spread: ***6 Hz***
- Delay Spread: ***1*** μs;
- Equivalent length of the guard time: ***22 samples***;
- Equivalent spacing of pulses during sounding : ***22 samples***;

Perfect modulation, demodulation, filtering and carrier recovery are assumed. Figure (5) shows the analytical performance of the 4-PSK and 8-PSK OM-DS-SS schemes with superimposed the simulation results.

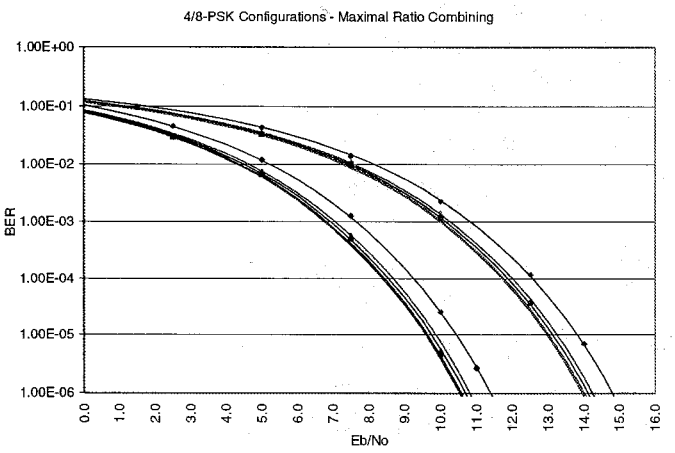

Fig. 5 BER Performance of 4-PSK and 8-PSK OM-DS-SS schemes for Maximal Ratio Combining. The curves are relative to analytical performance for S/D values of -10dB, -5dB, -2.5dB, 2.5dB. The dots are relative to the simulation results

Each set of curves shows the BER performance relative to S/D values of -10.0 dB, -5.0 dB, -2.5 dB and +2.5 dB. All curves refer to the ideal case of noiseless sounding. A good correspondence of analytical and simulation results may be observed. It can be noticed that curves relative to different values of the S/D ratio show clearly that the adoption of S/D values greater than -2.5 dB are not of use for better functioning since the BER performance improvement is negligible, while good performance is still obtained for an S/D value of -5dB. Regarding system performance in non linear environment, Figs. 6a and 6b show BER values versus the ratio of the bit energy over thermal noise spectral power. They refer to 4-PSK and 8-PSK signal mapping, respectively. Also, the simulation results are superimposed to the analytic curves in this case as well. For each back-off value, two curves are shown. The former is relative to noiseless sounding process, while the latter refers to the maximum value of the S/D parameter allowed for the considered value of the back-off. The first observation is that back-off values equal or greater than 6 dB do not produce a significant performance degradation if compared with the linear case. On the contrary, when back-off values are smaller, they induce a sensitive performance degradation. This effect is particularly evident in the case of 8-PSK constellation. In this case, the degradation becomes unacceptable (i.e. BER overcomes 1.0E-5 [1]) when back-off values are equal or lower than 3 dB. When 4-PSK constellation is adopted the minimum back-off acceptable is about 2 dB. In order to evaluate the optimum back-off value for a desired performance, the ratio between the penalty in terms of E_b/N_o due to the clipping effect and the gain in terms of IBO must be considered. For instance, in the case of the 8-PSK configuration, for obtaining a required

BER of 1.0E-5, the optimum back-off value of about 4 dB may be estimated.

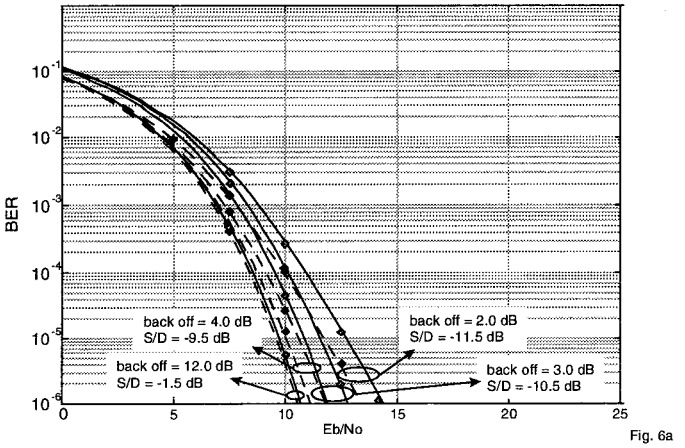

Fig. 6a

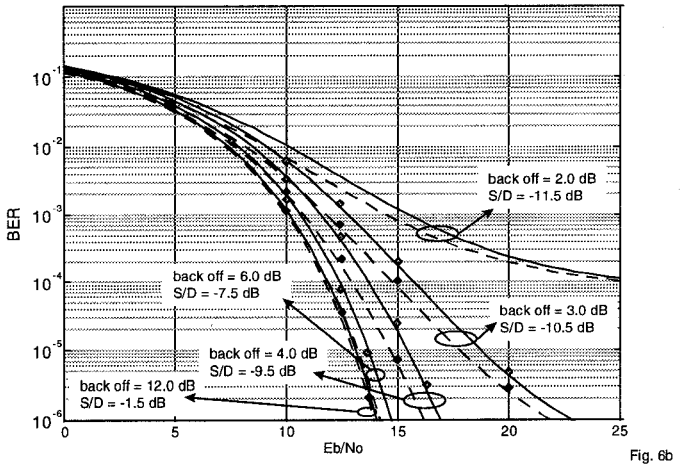

Fig. 6b

Fig. 6 BER performance versus E_b/N_0 of 4-PSK (6a) and 8-PSK (6b) OM-DS-SS schemes for Maximal Ratio Combining in clipping environment. The dashed curves are relative to analytical performance for noiseless sounding. The continuous curves are relative to analytical performance for the maximum S/D value allowed for a certain back off. The dots are relative to the simulation results.

Conclusions

In this paper an Orthogonal Multicarrier DS-SS radio access scheme for wireless LAN applications has been analysed in both linear and clipping environment. The analytical bit error rate performance and the simulation results for a realistic sounding technique and measured indoor channel delay profiles were reported. In the WLAN applications with CSMA/CA, the Orthogonal Multicarrier DS-SS radio access scheme represents an interesting technique to be adopted as it showed good performance in terms of BER and good capability of counteraction of multipath fading, which was also obtained for relatively low values of the S/D ratio. The analysis in the clipping environment permitted to estimate the system performance with a good approximation and also to specify the minimum back-off value for the various system configurations in order to balance the BER performance and the efficiency of power amplifiers.

References

[1] IEEE 802.11/D1, "Wireless LAN Medium Access Control (MAC) and Physical Layer (PHY) Specifications", *Draft Standard*, 1 December 1994.

[2] L. Goldberg, "MAC Protocols: The Key to Robust Wireless Systems", *Electronic Design*, vol.42, pp.63-74, 1994.

[3] B. Bourin, "HIPERLAN - Markets and Applications Standardisations Issues", *IEEE International Conference on Personal, Indoor and Mobile Radio Communications (PIMRC'94)*, Hague, Netherlands, 1994, pp. 863-868

[4] A. Falsafi, K. Pahlavan, "A Comparison Between the Performance of FHSS and DSSS for Wireless LANs Using a 3D Ray Tracing Program", *IEEE Vehicular Technology Conference (VTC'95)*, Chicago, USA, 1995, pp 569-573.

[5] A. Chouly, A. Brajal, S, Jourdan, "Orthogonal Multicarrier Technique applied to Direct Sequence Spread Spectrum CDMA systems" *IEEE GlobeCom, 1993*, pp. 1723-1728.

[6] N. Yee, J.P. M.G. Linnartz, G. Fettweis, "Multi-Carrier CDMA in Indoor Wireless Radio Networks", *IEICE Transactions on Communications*, vol. E77-B, July 1994.

[7] C. Reiners, H. Rohling, "Multicarrier Transmission Technique in Cellular Mobile Communication Systems", IEEE ", *IEEE Vehicular Technology Conference Proceedings (VTC'94)*, 1994, pp. 1645- 1649.

[8] L. Cimini, "Analysis and Simulation of a Digital Mobile Channel using Orthogonal Frequency Division Multiplexing", *IEEE Transactions on Communications*, vol. COM-33, pp. 665-675, July 1985.

[9] R. O'Neill, L.B Lopes, "Performance of Amplitude Limited Multitone Signals", in *IEEE Vehicular Technology Conference (IEEE VTC'94)*, June 1994, 1994, pp. 1675-1679.

[10] G. Santella, F. Mazzenga, "A Model for Performance Evaluation in M-QAM-OFDM Schemes in Presence of Nonlinear Distortions", *IEEE Vehicular Technology Conference (VTC'95)*, 1995, pp 830-834.

[11] S. Cacopardi, F. Frescura, F. Gatti, G. Reali "Channel Estimation and Tracking of an Indoor Orthogonal Multicarrier DS-CDMA System Using Measured Channel Delay Profiles", *IEEE Vehicular Technology Conference (IEEE VTC'96)*, 1996, pp. 1559-1563.

[12] S. Kaiser, "Analytical Performance Evaluation of OFDM-CDMA Mobile Radio Systems", *European Personal and Mobile Communications Conference (EPMCC'95)*, 1995, pp 215-220.

[13] A.R. Kaye, D.A. George, and M.J. Eric, "Analysis and Compensation of Bandpass Nonlinearity for Communications", *IEEE Transactions on Communications*, pp. 965-672, October 1972.

[14] D.J.G. Mestdagh, P. Spruyt, and B. Biran, " Analysis of Clipping Effects in DMT-Based ADSL Systems", *IEEE International Conference on Communications (ICC '94)*,1994, pp. 293-300.

[15] J. Rinne, and M. Renfors, "The Behaviour of Orthogonal Frequency Division Multiplexing Signals in Amplitude Limiting Channel" *IEEE International Conference on Communications (ICC '94)*,1994, pp. 381-385.

[16] R. Gross, and D. Veeneman, "SNR and Spectral Properties for a Clipped DMT ADSL Signal", *IEEE International Conference on Communications (ICC '94)*, 1994, pp. 843-847.

[17] R. E. Ziemer, R. L. Peterson, "Introduction to Digital Communication" *Macmillan Publishing Company*, 1992, pp. 297-301.